Stepping away from serendipity in Deep Eutectic Solvent formation: Prediction from precursors ratio

Francesco Cappelluti [a], Alessandro Mariani [b,c], Matteo Bonomo [d,e,*], Alessandro Damin [d], Luigi Bencivenni [e], Stefano Passerini [b,c], Marilena Carbone [f], Lorenzo Gontrani [e,f]

[a] *Institute of Structure of Matter – CNR, Area della Ricerca di Roma 1, 00015 Monterotondo Scalo, Italy*
[b] *Helmholtz Institute Ulm (HIU) for Electrochemical Energy Storage, Helmholtzstraße 11, 89081 Ulm, Germany*
[c] *Karlsruhe Institute of Technology (KIT), P.O. Box 3640, 76021 Karlsruhe, Germany*
[d] *Department of Chemistry, NIS Interdepartmental Centre and INSTM Reference Centre - University of Turin, Via Pietro Giuria 7, 10125 Turin, Italy*
[e] *Department of Chemistry - University of Rome "La Sapienza", P.le A. Moro 5, I-00185 Roma, Italy*
[f] *Department of Chemical Science and Technology - University of Rome "Tor Vergata", Via della Ricerca Scientifica 1, 00133 Rome, Italy*

Keywords:
DESs
X-ray scattering
Prediction
Molecular dynamics
Raman
Green Solvents

A B S T R A C T

Deep Eutectic Solvents (DESs) are a class of environment friendly and cheap solvents that are effectively employed in many different fields; nevertheless, a thorough elucidation of their structure is still lacking and the unambiguous categorization of a mixture as a DES is challenging. Throughout this paper, we develop a procedure based on computational tools (supported by experimental data) that could help in making a priori predictions of DESs formation. After validating the approach with X-ray scattering data, a series of aromatic molecules (as Hydrogen Bond Donor, HBD) was investigated to corroborate the method that could be potentially extended to other DESs. The computational findings evidenced a remarkable and unprecedented predictive power. Furthermore, as a bridge between computed and experimental data, a linear correlation between the calculated chloride-HBD coordination number and the decrease of the freezing temperature of the mixtures is found, being 0.7 a threshold value to obtain a liquid eutectic mixture at room temperature as further validated by experimental Raman spectra. This approach has been preliminary tested also with DESs based on alternative HBDs (*i.e.*, aliphatic alcohols, amines, and carboxylic acids), confirming the flexibility and the generality of the method.

1. Introduction

Deep Eutectic Solvents (DESs) are molecular systems characterized by a remarkably lower melting point if compared with their pristine components [1,2]. They have attracted increasing attention since their first description by Abbott *et al.* [3], because of their many valuable properties, such as the extreme chemical tunability and the low vapour pressure and flammability if compared to traditional organic solvents [4], making them somewhat similar to ionic liquids (ILs) [5]. The two latter features enable more accessible storage and employment making them a "greener" alternative to both organic solvents and ILs, even more, when referring to the sub-category of Natural DES (NaDES), for which the biocompatibility of all the mixture components is emphasized [6,7]. Moreover, DESs do not require an inert atmosphere for preparation and are considered not poisonous [8] (even though their absolute low toxicity has been debated [9]). The main application of DESs is, currently, in the fields of metal processing, [10] biomass pretreatment, [11] and biodiesel purification, [12] but very promising and environmentally meaningful applications concern CO_2 capture [13,14] as well as the development of next-generation batteries [15].

The general formula of these compounds is X^+Y^- nHBD, where X^+Y^- is an organic or inorganic salt and HBD stands for Hydrogen Bond Donor (*i.e.*, a Brønsted or Lewis acid). Recently, some other classes of DESs have been proposed avoiding the employment of salts and environmentally harmful metal ions and using multiple HBDs with different donor abilities [16]. In these approaches, liquid systems have been obtained but the molecular interactions ruling the formation of the systems have not been thoroughly investigated.

Since Abbott's pioneering paper, [3] one of the most widespread organic salts used is choline chloride (ChCl), that has the advantage of being very cheap (and it can even be extracted from biomass), non-toxic and biodegradable [17]. Moreover, its eutectic mixtures

can usually be prepared by straightforward mixing, avoiding any purification and waste disposal procedure. When screening the literature on DESs, one could note that plenty of different systems has been proposed, but their physical–chemical characterization is scarce or even absent, as most of the papers are focused on the final application.

Nevertheless, the determination of which systems could be considered a DES or not is still debated [2]. As a rule of thumb, forming a liquid mixture starting from two solid precursors could be considered a positive hint toward the formation of a eutectic system, but it might not be enough to prove its deepness. Moreover, when a liquid component is selected, discriminating between a DES or a "simple" salt-in-solvent mixture is quite challenging. Similar issues could arise from the presence of water in the DES mixture [18]. In the latter cases, the determination of actual DES formation is made *a posteriori* through spectroscopic, structural and electrochemical approaches [19–22]. Thus, although a "trial-and-error" approach could be valuable in some cases, the *a priori* determination of the DES formation from the mere knowledge of the starting components is of strategic importance and theoretical modelling is a fundamental tool. The number of computational studies on DESs is still limited, and this is quite unexpected, being their description usually less problematic compared to ILs [20,23,24]. Actually, when DESs are investigated with classical Molecular Dynamics (MD) simulations, a very good agreement with experimental data is obtained even without the use of the computationally expensive many-body force fields, likely because of the reduced overall charges on the fragments and the consequent decrease of the "computational viscosity" [25]. Nonetheless, great attention must be paid to the careful determination of the atomic charges [26]. Generic force fields such as the Generalized Amber Force Field (GAFF) [27], the Merck Molecular Force Field (MMFF) [28] and CHAMM Force Field [29] have been almost uniquely employed in these studies, even though the development of a dedicated one has been undertaken by Ullah *et al.* [30].

In the current study, we performed a screening of nine different mixtures composed of ChCl and phenol-derived molecules as HBDs (Fig. 1). Albeit some experimental studies on a limited set of phenols have already been performed [31,32], these papers are focused on the properties of the mixtures rather than on their structural elucidation. The selected series of phenols allows us to investigate the effect of the presence of multiple alcoholic moieties and if the insertion of an apolar substituent (*i.e.,* a methyl group) could impact the properties of the resulting mixture. The computational study includes classical MD simulations in order to assess the extent of DES formation for each mixture and, for their analysis, we decided to employ tools like Radial Distribution Function (RDF) calculations that do not require lengthy and computationally expensive simulations, such as those needed, for example, for the estimation of free energies of mixing [33]. The basis for these simulations is provided by the satisfactory agreement between theoretically predicted and experimentally measured structure factors.

The remarkable correlation found between computational and experimental evidence allows us to select some features to be exploited in the *a priori* prediction of DESs formation.

2. Result and discussion

2.1. Chemical characterization of Mixtures.

As a starting point of the analyses, we attempted the actual formulation of all the mixtures of the nine phenols (HBD) with the ChCl (HBA). Among the selected systems, the ones named **1-OH** and **1-OH-2-M** have particular importance because their formation has been already experimentally confirmed [31]. In both cases, an

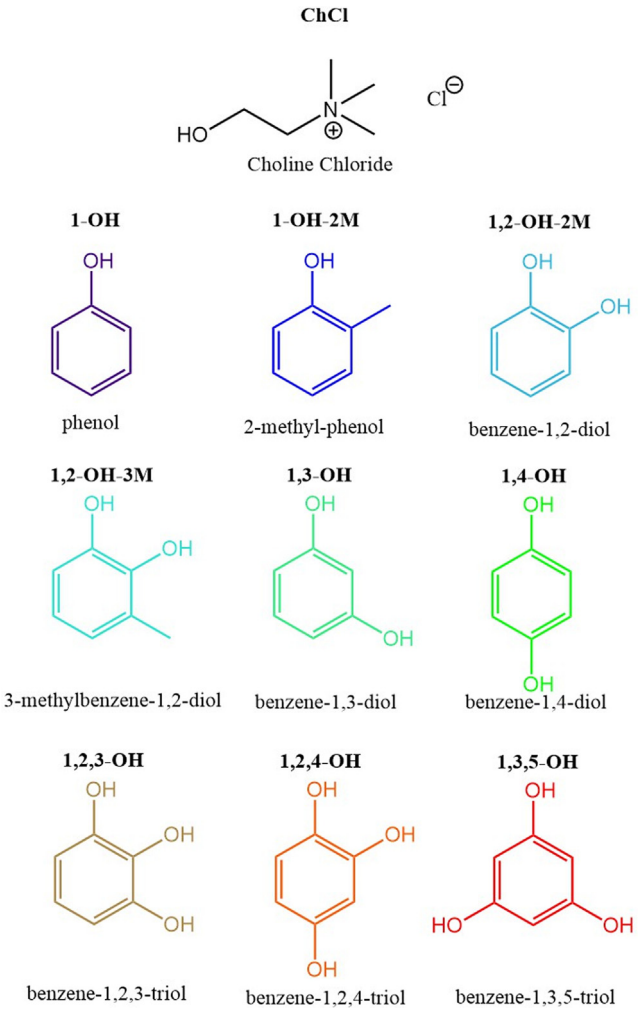

Fig. 1. Choline Chloride (as Hydrogen Bond Acceptor. HBA) and Phenol-derived Hydrogen Bond Donors investigated throughout this work.

HBD:HBA ratio equal to 3:1 was proposed. We decided to keep this value constant to reduce the number of variables to be considered in the comparative analyses. As expected, a unique behaviour was not found: some mixtures became a homogeneous liquid by simple mixing at room temperature, RT (*i.e.*, 298 K), some others needed a heating step (at 358 K) to speed up the kinetics of the process. A third set of mixtures did not (or just partially did) form a homogenous phase, accounting for a not optimal HBD:ChCl ratio. We are aware that the imposed ratio could not allow the formation of a DES or could lead to a not homogeneous mixture (these two scenarios could be expected when the total number of hydroxyl moieties of the HBD is increased), but the synthesis of new eutectic mixtures is out of the scope of the present paper.

The only DESs formed entirely at RT after simple mixing of the precursors are **1-OH** and **1-OH-2-M**; on the other hand, **1,2-OH**, **1,3-OH** and **1,2,3-OH** formed after gentle heating and remained liquid also when cooled down to room temperature. **1,3,5-OH** was not liquid (at least at T < 358 K) whereas the other mixtures became liquid after heating but (partially) solidified at room temperature, accounting for a "less deep" eutectic mixture or a not optimal stoichiometric ratio. Chemical composition of the mixtures have been elucidated by ^{1}H NMR spectroscopy (**Figure S1** and **Table S1**).

Once we proved that the investigated liquid mixtures had a fixed composition, even though a unique HBD:ChCl ratio could

not be found, (i) their eutectic behaviour and (ii) the "deepness" of their melting point (T_m) had to be assessed to establish whether they could be categorized as DESs or not. An "eutectic" mixture is characterized by a unique and well-defined melting temperature, which is, in turn, the lowest possible value. T_m values are summarized in **Table S2**. The experimental results do not allow us to use DSC to determine the T_m of all our mixtures. Therefore, we resolved to also use two other approaches (see the experimental section).

The concept of "deep" still does not have a largely agreed definition in the DES literature. In the pioneering paper by Abbott, the 1:2 ChCl:urea mixture was defined as "deep" being liquid even at temperature lower than RT (*i.e.*, 285 K) and having the eutectic a ΔT_m higher than 100 K compared to the precursor with the lowest T_m. The RT limit could, however, be highly misleading, though of high practical usefulness. In order to avoid any dependence on a single precursor, we defined the T_m depression values as the difference between the ideal melting temperature of the mixtures, defined from thermodynamics (see **equation S1**) [34,35].

After the initial investigation reported above, both **1-OH** and **1-OH-2-M** confirm their DES nature. On the other hand, **1,3,5-OH** does not even melt at the highest operating temperatures (T > 353 K). Therefore, these two extremes will be considered as references for DES and not-DES systems in the following analyses. Other mixtures, for example **1,2-OH**, present intermediate behaviour that should be further investigated before drawing any conclusion.

2.2. Small/Wide angle X-ray scattering (S-WAXS) analyses.

To shed more light on the structure of the obtained mixtures, we resolved to temperature-dependent S-WAXS measurements. X-ray patterns were recorded for all but two mixtures, namely **1,2,4-OH** and **1,3,5-OH**. The latter, being solid even at high temperature, makes the filling of the capillary impossible. Also, **1,2,4-OH** could not be inserted into the capillary since it immediately solidifies in contact with the glass walls causing its implosion. Among the seven experimental profiles reported (Fig. 2), five cases (**1-OH**, **1-OH-2-M**, **1,2-OH**, **1,3-OH** and **1,2,3-OH**) show the typical behaviour observed in most liquid samples that is characterized by large oscillations after a most prominent (main or "adjacency"

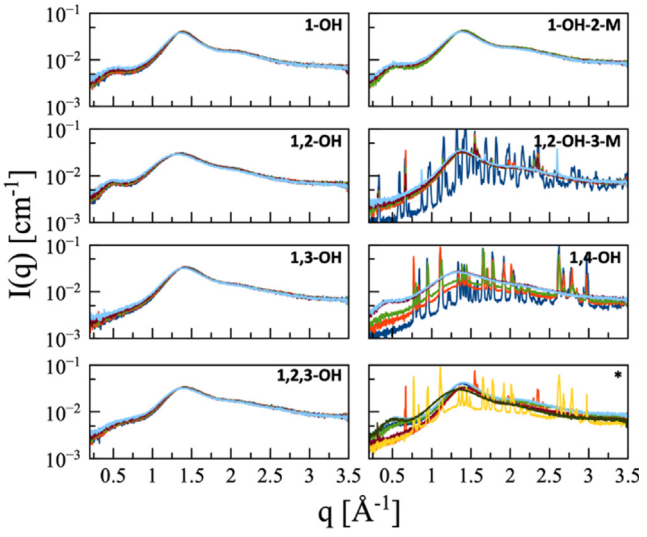

Fig. 2. Temperature dependent I(q). 283 K (blue); 303 K (red); 323 K (green); 343 K (brown); 363 K (cyan). The panel indexed with a star shows the comparison between different samples at 303 K. 1-OH (blue); 1,4-OH (red); 1,2,3-OH (green); 1,3-OH (brown); 1-OH-2-M (cyan); 1,2-OH-3-M (yellow); 1,2-OH (dark green).

[36]) peak, mainly originated by intermolecular correlations. This peak position for the samples liquid at RT, along with the corresponding characteristic distance, are reported in **Table S3**. Except for **1,2-OH**, all the systems show a very similar peak position, indicating comparable first solvation shells, which could be expected since all the mixtures contain similar molecules. The exceptional low q value for the main peak of **1,2-OH** is probably linked to the hydrogen bonding sites being in the ortho position, inducing a more compact packing of the surrounding molecules.

The peak width(s) is related to the large number of different local structural arrangements overlying such an average correlation. In four cases (**1-OH**, **1-OH-2-M**, **1,2-OH** and **1,2,3-OH**), an additional low-intensity feature is visible in the patterns around 0.3 Å^{-1}, more clearly defined in **1-OH**, **1-OH-2-M** and **1,2-OH**. This peak, often termed as "First Sharp Diffraction Peak" (FSDP) or pre-peak, is typically linked to the establishment of intermediate-range order in the bulk. Its observation has been related to different long range structural motifs, ranging from the self-segregated domains of different charge/polarity [37] in ILs [38] and molecular liquids [39] to other kinds of mesoscale aggregation or network formation [40,41], as in some inorganic glasses [42]. In two samples (**1,2-OH-3-M** and **1,4-OH**), that are solid at RT, the measured patterns are quite different and show a crystalline powder-like aspect, with a higher amorphous phase content in **1,4-OH**, where the crystalline peaks emerge from the underlying continuous envelope. The principal peak observed in the liquid systems could be regarded as resulting from the "melting" of the crystal peaks underneath [43]. The putative conversion of some crystal peaks into pre-peak is less straightforward and could be hypothesized for **1,4-OH** only, since no pre-peak is visible in **1,2-OH-3-M,** at least at 363 K, the highest temperature investigated; the peaks visible around 0.7 Å^{-1} in **1,4-OH** appear too far from the reciprocal distance of the pre-peak, and this points to a different structural arrangement in the solid than in the liquid.

Concerning the temperature dependency of the structure, the five RT-DES show the usual and expected behaviour for both the main peak and the pre-peak (when present), *i.e.*, a marked shifting toward smaller q values with increasing temperature. This is simply because of the volume expansion induced by the heating process. However, the two samples solid at RT depict a more complex scenario. While **1,2-OH-3-M** never melts completely, as witnessed by the presence of Bragg peaks even at the highest explored temperature, **1,4-OH** is a proper liquid at 343 K. Very interestingly, this sample develops the pre-peak once liquified, even if no crystalline peaks were observed in the solid phase at that q region. Further investigation on this peculiar phenomenon is required, and it will be discussed in a future work.

2.3. S-WAXS-steered molecular dynamics as a diagnostic tool.

Once we collected a solid dataset of experimental data, we took advantage of computational tools, simulating the systems and extracting the corresponding structure factors [44,45]. The comparison between experimental (dashed lines) and computed (solid lines) patterns is shown in **Figure S3**, in the 0.2–5 Å^{-1} range. The good agreement between the experimental and the computed structure factors (S(q)) proves the accurate description that classical MD can provide for DESs [20,46], validating our following analyses. The only disagreement can be noticed in the overestimation of the pre-peak at low q, signalling that the simulated system is too ordered at a mesoscopic level compared to the real mixture.

A powerful feature of the structure factors derived from simulations is the possibility of decomposing them into contributions coming from atomic subsets. This is, on the contrary, impossible when dealing with experimental X-ray patterns. In Fig. 3, the contributions given by the HBD moieties alone to the computed S(q)s

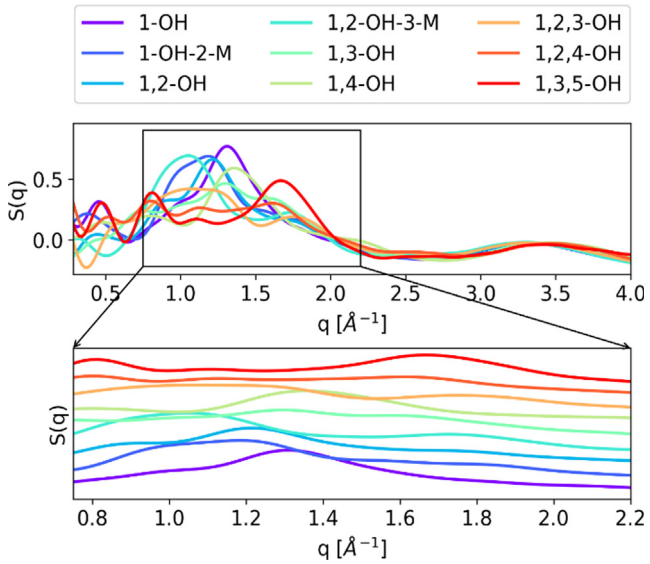

Fig. 3. S(q) contribution of HBD-HBD interactions to the total S(q). In the inset, the region 0.75–2.2 Å^{-1} is reported to evidence the intermolecular structural contributions that give origin to the main peak of the structure factor. In the inset, curves are vertically shifted for sake of clarity.

are shown in the range 0.025–4 Å^{-1}. The latter threshold corresponds to about 1.6 Å in real space, whereas 0.025 Å^{-1} limit is imposed by the size of the simulation cell. We resolved to employ the "atomic" S(q) structure factor instead of I(q) (connected by the relation $I(q)/\sum_i(x_i{*}f_i)^2$) because the normalization of the former by the self-scattering term constitutes a clear advantage when comparing functions referred to systems with different "electronic" content, such as the ones hereafter discussed, by permitting to only focus on the structural contributions [47].

The most interesting region (inset of Fig. 3) is located between 0.75 and 2.2 Å^{-1} (corresponding, in direct space, to a 2.9–8 Å range) and contains the intermolecular structural contributions that give origin to the main peak of the structure factor [36]. Significant differences exist in this region between the structure factors of the nine mixtures, and it can be observed that, with some exceptions, the position of the peak roughly relates to the degree of substitution of the aromatic ring of the HBDs. Since, as previously discussed, the formation of the DES can be undoubtedly asserted for **1-OH**, **1-OH-2-M**, (and ruled out for **1,3,5-OH**), a main peak shifted to the left can be proposed as a clue for predicting this. A further corroboration to this finding comes from the inspection of the computed S(q) of **1,2,3-OH**: even though this phenol is highly functionalized, its main peak is shifted to the left, and the experiments indeed show that its mixture with ChCl melts after gentle heating.

The partial structure factors generated by the other components of the mixture (*i.e.*, choline and chloride) and the contributions coming from the three possible pairs of the moieties (*i.e.*, HBD-choline, HBD-chloride and choline-chloride) are reported in **Figure S4**.

The most noticeable feature observed in the plots is the relevant contribution to the pre-peak (when present) coming from the choline and mixed choline-chloride partial structure factors. This evidence perfectly correlates with the findings already reported by some of us [20], in which a moderate persistence of the ChCl electrostatic interaction played a pivotal role in the stabilization of the DES. Having identified the pre-peak as a structural feature typical of the mixtures forming a DES, this finding shows the importance of the long-range ordering imposed by ChCl.

Aiming at disclosing the nature of the investigated mixtures, we resolved to investigate RDFs (or g(r)s): this is a powerful tool for inspecting the structure of a system and calculating the coordination number of a given atom type. To compare RDFs from different systems and avoid artefacts coming from the different densities of the simulation boxes, we multiplied them by the number density of the observed system [48,49]. So, strictly speaking, the displayed RDFs are (g(r)·ρ)s. RDFs between the centres of the aromatic ring (COR) of HBDs and the centres of mass (COM) of choline molecules, HBD-HBD RDF and Ch^+–Ch^+ RDF, are depicted in **Figure S5-S10** and thoroughly discussed in the Supporting Information. To shed light on the distinct hydrogen-bond network, we performed an RDF analysis of the $O_{HBD}\cdots Cl^-$ interaction to gain information about the mixing (or, conversely, the segregation) of DES components. RDFs and first peak integrals for $O_{HBD}\cdots Cl^-$ pair are shown in the left and right upper panels of Fig. 4, respectively. Independently of the nature of the HBD, all mixtures presented a peak centred at 2.7–2.9 Å, which is compatible with the typical hydrogen bonds involving halide anions [50]. For **1-OH** and **1-OH-2-M**, integral values quite close to one are observed.

The latter decreases for di-hydroxyl (0.8–0.6) and tri-hydroxyl (0.6–0.4) substituted HBDs. Furthermore, a dependence on the position of the additional hydroxyl moiety(ies) could also be noticed, with ortho- substituents more strongly coordinating than para- and meta- ones. This effect is ascribable to the rigidity of the aromatic ring that almost completely prevents different hydroxyl groups (of the same ring) from coordinating the same chloride ion, except for *ortho*-substituted HBDs (**Figure S11**). Since $O_{HBD}\cdots Cl^-$ bonding is supposed to be at the basis of the DES formation, it would be significant to correlate the calculated integral value with other experimental evidence (*vide infra*).

As already experimentally proven for other DESs, the partial preservation of $N_{Ch}\cdots Cl^-$ interaction (bottom left panel of Fig. 4) could be helpful in the mixture stabilization [22]. Two peaks can be appreciated: the former and more intense is located at a distance slightly longer than 4 Å. The latter, instead, lies before 6 Å. The use of molecular mechanics' models (**Figure S12-S13**) permitted to connect the first peak to both $N_{Ch}\cdots Cl^-$ and $O_{Ch}\cdots Cl^-$ interactions. Such a conclusion is strengthened by the presence of a shoulder on the right of the main peak in almost all cases, probably connected to the chloride ions interacting with the alcoholic hydrogen. One should note that these interactions could take place in DES, as well as in salt-in-solvent mixtures. On the other hand, the peak located slightly before 6 Å could not be easily rationalized using the simple molecular mechanics' models previously employed. The inspection of a few frames from the MD trajectories (**Figure S14**) revealed that such a relatively long-distance correlation between the oppositely charged Cl^- and N^+ could only be realized owing to the presence of a considerable number of alcoholic groups from several residues lying in between. This intuition is corroborated by the inspection of the changes in the RDF when varying the degree of substitution of the aromatic ring: the intensity of the first peak is roughly inversely proportional to that of the second one when going from **1-OH** to **1,3,5-OH**.

Finally, the intermolecular $O_{HBD}\cdots O_{HBD}$ RDFs were calculated (lower right panel of Fig. 4). By focusing on the short-range part, two peaks can be generally observed: the first, at about 3 Å, can be associated with a direct hydrogen bond between two HBDs. The intensity of this peak could be inversely related to the formation of a DES, being the eutectic mixture characterized by the presence of hydroxyl moieties (almost) utterly involved in the coordination (*i.e.,* stabilization) of the Cl^- more than in homologous interaction. As a rule of thumb, it could be reasonably expected that a DES could be formed when $O_{HBD}\cdots Cl^-\cdots O_{HBD}$ interactions are favoured over $O_{HBD}\cdots O_{HBD}$ ones. From this assumption, it seems evident that in **1,2,4-OH** and **1,2,5-OH**, the HBD-HBD interactions still play a relevant role, likely preventing the DES formation. A fainter (**1-OH-2-M** and **1,2-OH-3-M**) or absent (**1-OH** and **1,2-**

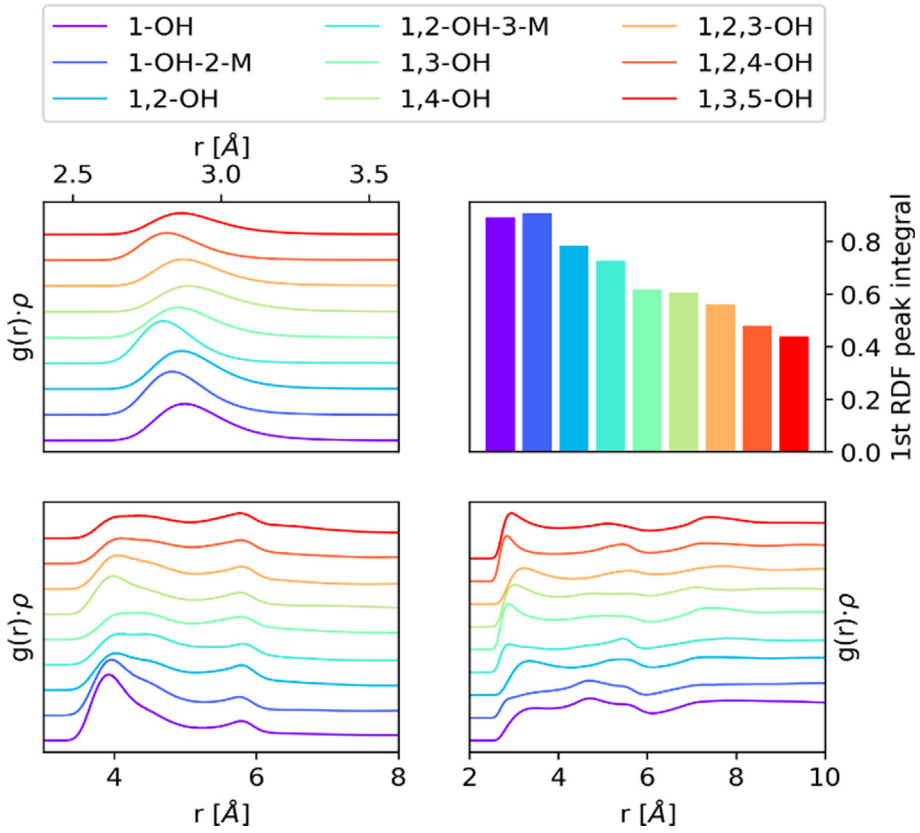

Fig. 4. Top left: $O_{HBD}\cdots Cl^-$ radial distribution function. Top right: first peak integral of $O_{HBD}\cdots Cl^-$ radial distribution function - . Bottom left: Ch-$N^+\cdots Cl^-$ radial distribution function. Bottom right: $O_{HBD}\cdots O_{HBD}$ radial distribution function. The RDFs are vertically shifted for the sake of clarity.

OH) peak accounts for reduced (or absent) interactions, whereas a peak shifted toward longer distances is ascribable to slackened ones. Additionally, the presence of a methyl substituent could partially prevent the packing of the HBD molecules due to steric hindrance. The second peak, located around 5 Å, has been interpreted, with the help of the CDFs correlating Cl···HBD COR distance and the angle HBD_{COR}-Cl-HBD'_{COR} (Figure S7) and the visual inspection of a few trajectory frames, as a structure having a chloride ion acting as an almost linear bridge between two alcoholic groups. Other interpretations, such as π-π stacking phenomena, could not be completely ruled out.

2.4. Correlation between melting temperature depletion and computed RDF integral

Very interestingly, the values of the freezing-point depression of different DESs (listed in **Table S2**) correlate remarkably well with the value of the integral of the $O_{HBD}\cdots Cl^-$ interaction (Fig. 4, top right frame), if the T_m depression for **1,3-OH** is excluded. This correlation is shown in the upper panel of Fig. 5. Indeed, the higher the coordination number C_N, the higher the ΔT_m (*i.e.*, the "deepest" the eutectic mixture). More precisely, a linear dependence could be extracted obeying the following equation: $\Delta T_m = a + k\, C_N$, in which ΔT_m is the average between the freezing-point depressions measured with the different (available) approaches, C_N is the coordination number of Cl^-, k (>0) is the proportionality constant and a is the intercept of the model. Notwithstanding the remarkable correlation found, we decided to further validate the model by exploiting Raman spectroscopy. In fact, this technique allowed us to select some paramount vibrational modes that would be sizeably affected by the potential formation of a DES mixture and to follow their evolution in the investigated systems: this because frequencies associated to vibrational modes of a molecule can be strongly affected just by the local environment, as it is the case for CO, N_2 and H_2 probe molecules widely adopted for surfaces characterization [51].

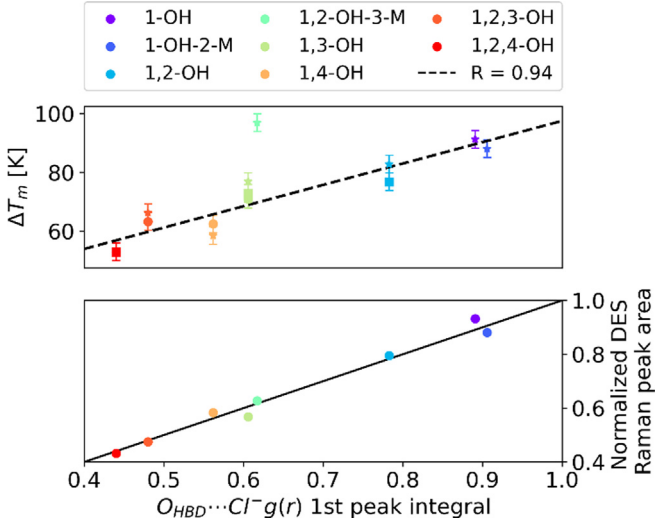

Fig. 5. Correlation between $O_{HBD}\cdots Cl^-$ interaction and ΔT_m of mixtures (upper panel) and ratio of integrated areas of Raman peaks (lower panel). The ΔT_m values obtained from DSC measurement are plotted using stars, those obtained from thermometer measurements using squares and those obtained from capillary tube measurements using circles (see experimental section for details on the three methods). Dotted line in upper panel is the result of the interpolation; solid line in the lower panel corresponds to the bisector of the first quadrant and it should be understood as a guide for the readers' eye.

When case system **1-OH** is concerned, the above assumption is strongly corroborated by the comparison of Raman spectrum recorded on its solid form (close packed molecules forming OH···-OH chains) with data coming from literature and obtained in the gas phase (isolated molecule) [52]: as it can be seen, n_{COH} undergoes a significant red-shift on passing from the gas phase (dotted black line in **Figure S15**) to the solid one (solid blue line in **Figure S15**). The trend is also supported by Raman spectra computed at DFT level on isolated phenol and on its trimers.

Therefore, Raman spectra of 3:1 mixtures have been collected and compared to the ones of the precursors (both HBDs and ChCl) as reported in **Figure S16**. From the inspection of the latter, it is quite clear that the spectra of the mixtures cannot be simply attributed to a mechanical mixing of the two components in the proper stoichiometric ratio. Moreover, some remarkable changes could be detected in the band located in regions nearby 1050 (d_{CH}), 1250 (n_{COH}) and 1620 cm^{-1} (n_{CC}), respectively (see **Figure S15** for a graphical representation), where new contributions arise following on from the (partial) formation of the DES (**Figure S17**). The deconvolution of the bands allows separating the contribution of the pristine interaction (already present in the solid HBDs) and the ones arising from the DES formation. The ratio between the integrated areas could provide a fair indication of the formation degree for each system, and a noteworthy correlation with the value of the integral of the $O_{HBD}\cdots Cl^-$ interaction is shown in the lower panel of Fig. 5. For sake of truth, it should be pointed out that the position of the HB-like interaction band is invariant when partially formed system are investigated whereas it could vary (<5 cm^{-1}) when pure DES are investigated. This is likely due to the severe modification of the chemical environment experimented by the precursors resulting from the formation of the eutectic mixture. The found correlation further stresses that the $O_{HBD}\cdots$ Cl^- interaction and its magnitude underlie the DES formation, being C_N = 0.7 an empirical threshold for the obtainment of liquid DESs at RT. The latter correspond to a ΔT_m equal to 75 K that could be considered as the minimal melting point depression to consider a system as a DES.

We questioned the generality of our approach towards a larger set of DES not based on phenol-like precursors, thus we made the same analyses for a set of commonly studied deep eutectic solvents. We considered the systems obtained by mixing choline chloride with either urea, ethylene glycol or malonic acid, at two different HBD:HBA ratios, namely the eutectic composition (as reported in the literature) and one far from the eutectic point. This selection allows us to prove, at first, the proposed method with systems with different HBDs (*i.e.,* amides, aliphatic alcohols, and carboxylic acids). Our simulations found that all DES composition have an $O_{HBD}\cdots$Cl- 1st peak integral falling at values > 0.7, whereas for the non-eutectic composition the 1st peak integral was much lower than the threshold (see **Table S5** and **Figure S18**). To further widen the applicability of the proposed model (ruling out the mandatory presence of Cl^-, e.g., type-V DES) and established that the solvation energy of the HBA is the driving factor for the DES stabilization, we speculate that extracting this energy value from the simulation could return a system-independent threshold indicating the DES formation. Such an approach will be exploited in a forthcoming work.

3. Conclusion

Throughout this paper, we characterize nine different mixtures composed of phenols and choline chloride with a fixed 3:1 molar ratio, aiming at discriminating whether the formation of a DES occurs. The multi-technique approach proposed, based on thermal and spectroscopic measurements, allows us to undoubtedly categorize **1-OH**, **1-OH-2-M** and **1,2-OH** as DES and **1,3,5-OH** as a simple mixture of precursors. Once a reliable dataset of experimental results was obtained, we resolved to some computational studies (*i.e.* RDFs) to individuate specific features that could help in the a priori prediction of the formation of a DES, paving the way to a more thoughtful and efficient design of new systems. A series of pieces of evidence has been identified as a green light for the DES formation: (i) the presence of the pre-peak at 0.3 $Å^{-1}$, slightly overestimated in the simulation, accounting for a long-range order; (ii) the shift of the main peak of the partial HBD structure factor to low q values; (iii) the partial persistence of the $Ch^+\cdots Cl^-$ interaction, leading to a homogeneous structuration; (iv) a high value (close to 1) of the integral of the O_{HBD}-Cl^- interaction, highlighting the importance of the anion stabilization due to the hydrogen bond networking. To further correlate experimental and computed data, we found an almost perfect linear correlation between the ΔT_m and the $O_{HBD}\cdots Cl^-$ interaction: a value of 0.7 is a threshold for the mixture to be categorized as a DES at RT. These noteworthy results make us confident that a well-tuned simulation method, where the force field used to calculate the energetics of the system is thoroughly validated with structural data (diffraction patterns) coupled with quite unexpensive (RDFs) trajectory post-processing analyses, can be used as a powerful tool to predict the formation and to investigate the structure of a DES mixture comprehensively. Indeed, we are firmly convinced that the approach used in this paper for a specific series of phenols could be fairly transposed to a more extensive set of DESs, as proved by some experimental and computed data for some common ChCl-based DESs.

Materials and Methods

All the experimental and computational details with related reference and discussion can be found in the Supporting Information.

CRediT authorship contribution statement

Francesco Cappelluti: Data curation, Formal analysis, Investigation, Software, Visualization, Writing – original draft. **Alessandro Mariani:** Data curation, Formal analysis, Investigation, Methodology, Software, Visualization, Writing – original draft. **Matteo Bonomo:** Conceptualization, Data curation, Formal analysis, Investigation, Methodology, Project administration, Supervision, Writing – original draft, Writing – review & editing. **Alessandro Damin:** Data curation, Formal analysis, Investigation, Software, Visualization, Writing – original draft. **Luigi Bencivenni:** Methodology, Resources, Validation, Writing – review & editing. **Stefano Passerini:** Funding acquisition, Resources, Writing – review & editing. **Marilena Carbone:** Funding acquisition, Resources, Validation, Writing – review & editing. **Lorenzo Gontrani:** Conceptualization, Funding acquisition, Methodology, Project administration, Resources, Software, Supervision, Writing – original draft, Writing – review & editing.

Data availability

Data will be made available on request.

Declaration of Competing Interest

The authors declare that they have no known competing financial interests or personal relationships that could have appeared to influence the work reported in this paper.

Acknowledgements

Computer simulations have been performed on Galileo-HPC from Cineca under grant IscraC FRESP4IL. A.M. and S.P. acknowl-

edge the basic funding from the Helmholtz association and the Bundesministerium für Wissenschaft und Forschung (BMWi - FZK 03ETB003A). F. Cappelluti and A. Mariani contributed equally to this work. Miss Barbara Centrella is gratefully acknowledged for the realization of ToC.

Appendix A. Supplementary material

Supplementary data to this article can be found online at https://doi.org/10.1016/j.molliq.2022.120443.

References

[1] Q. Zhang, K. De Oliveira Vigier, S. Royer, F. Jérôme, Deep eutectic solvents: Syntheses, properties and applications, Chem. Soc. Rev. 41 (2012) 7108–7146, https://doi.org/10.1039/c2cs35178a.
[2] B.B. Hansen, S. Spittle, B. Chen, D. Poe, Y. Zhang, J.M. Klein, A. Horton, L. Adhikari, T. Zelovich, B.W. Doherty, B. Gurkan, E.J. Maginn, A. Ragauskas, M. Dadmun, T.A. Zawodzinski, G.A. Baker, M.E. Tuckerman, R.F. Savinell, J.R. Sangoro, Deep Eutectic Solvents: A Review of Fundamentals and Applications, Chem. Rev. 121 (2021) 1232–1285, https://doi.org/10.1021/acs.chemrev.0c00385.
[3] A.P. Abbott, G. Capper, D.L. Davies, H.L. Munro, R.K. Rasheed, V. Tambyrajah, Preparation of novel, moisture-stable, lewis-acidic ionic liquids containing quaternary ammonium salts with functional side chains, Chem. Commun. 1 (2001) 2010–2011, https://doi.org/10.1039/b106357j.
[4] E.L. Smith, A.P. Abbott, K.S. Ryder, Deep Eutectic Solvents (DESs) and Their Applications, Chem. Rev. 114 (2014) 11060–11082, https://doi.org/10.1021/cr300162p.
[5] R.D. Rogers, K.R. Seddon, Ionic Liquids - Solvents of the Future?, Science (80-,) 302 (2003) 792–793, https://doi.org/10.1126/science.1090313.
[6] Y. Dai, J. van Spronsen, G.J. Witkamp, R. Verpoorte, Y.H. Choi, Natural deep eutectic solvents as new potential media for green technology, Anal. Chim. Acta. 766 (2013) 61–68, https://doi.org/10.1016/j.aca.2012.12.019.
[7] L. Benvenutti, A.A.F. Zielinski, S.R.S. Ferreira, Which is the best food emerging solvent: IL, DES or NADES?, Trends Food Sci Technol. 90 (2019) 133–146, https://doi.org/10.1016/j.tifs.2019.06.003.
[8] B. Kudłak, K. Owczarek, J. Namieśnik, Selected issues related to the toxicity of ionic liquids and deep eutectic solvents—a review, Environ. Sci. Pollut. Res. 22 (2015) 11975–11992, https://doi.org/10.1007/s11356-015-4794-y.
[9] M. Hayyan, M.A. Hashim, A. Hayyan, M.A. Al-Saadi, I.M. AlNashef, M.E.S. Mirghani, O.K. Saheed, Are deep eutectic solvents benign or toxic?, Chemosphere 90 (2013) 2193–2195, https://doiorg/10.1016/j.chemosphere.2012.11.004.
[10] A.P. Abbott, G. Frisch, S.J. Gurman, A.R. Hillman, J. Hartley, F. Holyoak, K.S. Ryder, Ionometallurgy: Designer redox properties for metal processing, Chem. Commun. 47 (2011) 10031–10033, https://doi.org/10.1039/c1cc13616j.
[11] Y. Chen, T. Mu, Application of deep eutectic solvents in biomass pretreatment and conversion, Green Energy Environ. 4 (2019) 95–115, https://doi.org/10.1016/j.gee.2019.01.012.
[12] M. Hayyan, F.S. Mjalli, M.A. Hashim, I.M. AlNashef, A novel technique for separating glycerine from palm oil-based biodiesel using ionic liquids, Fuel Process. Technol. 91 (2010) 116–120, https://doi.org/10.1016/j.fuproc.2009.09.002.
[13] Y. Zhang, X. Ji, X. Lu, Choline-based deep eutectic solvents for CO2 separation: Review and thermodynamic analysis, Renew. Sustain. Energy Rev. 97 (2018) 436–455, https://doi.org/10.1016/j.rser.2018.08.007.
[14] L.L. Sze, S. Pandey, S. Ravula, S. Pandey, H. Zhao, G.A. Baker, S.N. Baker, Ternary deep eutectic solvents tasked for carbon dioxide capture, ACS Sustain. Chem. Eng. 2 (2014) 2117–2123, https://doi.org/10.1021/sc5001594.
[15] M.E. Di Pietro, A. Mele, Deep eutectics and analogues as electrolytes in batteries, J. Mol. Liq. 338 (2021), https://doi.org/10.1016/j.molliq.2021.116597 116597.
[16] D.O. Abranches, M.A.R. Martins, L.P. Silva, N. Schaeffer, S.P. Pinho, J.A.P. Coutinho, Phenolic hydrogen bond donors in the formation of non-ionic deep eutectic solvents: The quest for type v des, Chem. Commun. 55 (2019) 10253–10256, https://doi.org/10.1039/c9cc04846d.
[17] K. Radošević, M. Cvjetko Bubalo, V. Gaurina Srček, D. Grgas, T. Landeka Dragičević, R.I. Redovniković, Evaluation of toxicity and biodegradability of choline chloride based deep eutectic solvents, Ecotoxicol. Environ. Saf. 112 (2015) 46–53, https://doi.org/10.1016/j.ecoenv.2014.09.034.
[18] L.K. Savi, D. Carpiné, N. Waszczynskyj, R.H. Ribani, C.W.I. Haminiuk, Influence of temperature, water content and type of organic acid on the formation, stability and properties of functional natural deep eutectic solvents, Fluid Phase Equilib. 488 (2019) 40–47, https://doi.org/10.1016/j.fluid.2019.01.025.
[19] N. Delgado-Mellado, M. Larriba, P. Navarro, V. Rigual, M. Ayuso, J. García, F. Rodríguez, Thermal stability of choline chloride deep eutectic solvents by TGA/FTIR-ATR analysis, J. Mol. Liq. 260 (2018) 37–43, https://doi.org/10.1016/j.molliq.2018.03.076.
[20] L. Gontrani, N.V.V. Plechkova, M. Bonomo, In-Depth Physico-Chemical and Structural Investigation of a Dicarboxylic Acid/Choline Chloride Natural Deep Eutectic Solvent (NADES): A Spotlight on the Importance of a Rigorous Preparation Procedure, ACS Sustain. Chem. Eng. 7 (2019) 12536–12543, https://doi.org/10.1021/acssuschemeng.9b02402.
[21] M. Gilmore, L.M. Moura, A.H. Turner, M. Swadźba-Kwaśny, S.K. Callear, J.A. McCune, O.A. Scherman, J.D. Holbrey, A comparison of choline:urea and choline:oxalic acid deep eutectic solvents at 338 K, J. Chem. Phys. 148 (2018) 193823. doi:10.1063/1.5010246.
[22] M. Bonomo, L. Gontrani, A. Capocefalo, A. Sarra, A. Nucara, M. Carbone, P. Postorino, D. Dini, A combined electrochemical, infrared and EDXD tool to disclose Deep Eutectic Solvents formation when one precursor is liquid: Glyceline as case study, J. Mol. Liq. 319 (2020), https://doi.org/10.1016/j.molliq.2020.114292 114292.
[23] S.L. Perkins, P. Painter, C.M. Colina, Experimental and Computational Studies of Choline Chloride-Based Deep Eutectic Solvents, J. Chem. Eng. Data. 59 (2014) 3652–3662, https://doi.org/10.1021/je500520h.
[24] Z. Naseem, R.A. Shehzad, A. Ihsan, J. Iqbal, M. Zahid, A. Pervaiz, G. Sarwari, Theoretical investigation of supramolecular hydrogen-bonded choline chloride-based deep eutectic solvents using density functional theory, Chem. Phys. Lett. 769 (2021), https://doi.org/10.1016/J.CPLETT.2021.138427 138427.
[25] D. Bedrov, J.-P. Piquemal, O. Borodin, A.D. MacKerell, B. Roux, C. Schröder, Molecular Dynamics Simulations of Ionic Liquids and Electrolytes Using Polarizable Force Fields, Chem. Rev. 119 (13) (2019) 7940–7995.
[26] G. García, M. Atilhan, S. Aparicio, The impact of charges in force field parameterization for molecular dynamics simulations of deep eutectic solvents, J. Mol. Liq. 211 (2015) 506–514, https://doi.org/10.1016/j.molliq.2015.07.070.
[27] J. Wang, R.M. Wolf, J.W. Caldwell, P.A. Kollman, D.A. Case, Development and testing of a general Amber force field, J. Comput. Chem. 25 (2004) 1157–1174, https://doi.org/10.1002/jcc.20035.
[28] T.A. Halgren, Merck molecular force field. I. Basis, form, scope, parameterization, and performance of MMFF94, J. Comput. Chem. 17 (1996) 490–519, https://doi.org/10.1002/(SICI)1096-987X(199604)17:5/6<490::AID-JCC1>3.0.CO;2-P.
[29] S. Kaur, A. Malik, H.K. Kashyap, Anatomy of Microscopic Structure of Ethaline Deep Eutectic Solvent Decoded through Molecular Dynamics Simulations, J. Phys. Chem. B. 123 (2019) 8291–8299, https://doi.org/10.1021/acs.jpcb.9b06624.
[30] R. Ullah, M. Atilhan, B. Anaya, M. Khraisheh, G. García, A. Elkhattat, M. Tariq, S. Aparicio, A detailed study of cholinium chloride and levulinic acid deep eutectic solvent system for CO2capture via experimental and molecular simulation approaches, Phys. Chem. Chem. Phys. 17 (2015) 20941–20960, https://doi.org/10.1039/c5cp03364k.
[31] W. Guo, Y. Hou, S. Ren, S. Tian, W. Wu, Formation of deep eutectic solvents by phenols and choline chloride and their physical properties, J. Chem. Eng. Data. 58 (2013) 866–872, https://doi.org/10.1021/je300997v.
[32] J. Zhu, K. Yu, Y. Zhu, R. Zhu, F. Ye, N. Song, Y. Xu, Physicochemical properties of deep eutectic solvents formed by choline chloride and phenolic compounds at T = (293.15 to 333.15) K: The influence of electronic effect of substitution group, J. Mol. Liq. 232 (2017) 182–187. doi:10.1016/j.molliq.2017.02.071.
[33] N. Hansen, W.F. Van Gunsteren, Practical aspects of free-energy calculations: A review, J. Chem. Theory Comput. 10 (2014) 2632–2647, https://doi.org/10.1021/ct500161f.
[34] M.A.R. Martins, S.P. Pinho, J.A.P. Coutinho, Insights into the Nature of Eutectic and Deep Eutectic Mixtures, J. Solution Chem. 48 (2019) 962–982, https://doi.org/10.1007/s10953-018-0793-1.
[35] L.J.B.M. Kollau, M. Vis, A. Van Den Bruinhorst, A.C.C. Esteves, R. Tuinier, Quantification of the liquid window of deep eutectic solvents, Chem. Commun. 54 (2018) 13351–13354, https://doi.org/10.1039/c8cc05815f.
[36] J.C. Araque, J.J. Hettige, C.J. Margulis, Modern Room Temperature Ionic Liquids, a Simple Guide to Understanding Their Structure and How It May Relate to Dynamics, J. Phys. Chem. B. 119 (2015) 12727–12740, https://doi.org/10.1021/acs.jpcb.5b05506.
[37] M. Campetella, S. De Santis, R. Caminiti, P. Ballirano, C. Sadun, L. Tanzi, L. Gontrani, Is a medium-range order pre-peak possible for ionic liquids without an aliphatic chain?, RSC Adv 5 (2015) 50938–50941, https://doi.org/10.1039/c5ra07567j.
[38] A. Mariani, R. Caminiti, M. Campetella, L. Gontrani, Pressure-induced Mesoscopic Disorder in Protic Ionic Liquids: First Computational Study, Phys. Chem. Chem. Phys. 18 (2016) 2297–2302, https://doi.org/10.1039/C5CP06800B.
[39] A. Perera, Charge ordering and scattering pre-peaks in ionic liquids and alcohols, Phys. Chem. Chem. Phys. 19 (2017) 1062–1073, https://doi.org/10.1039/c6cp07834f.
[40] I. Pethes, L. Temleitner, M. Tomšič, A. Jamnik, L. Pusztai, X-Ray Diffraction and Computer Simulation Studies of the Structure of Liquid Aliphatic Aldehydes: From Propanal to Nonanal, Phys. Status Solidi Basic Res. 255 (2018) 1800127, https://doi.org/10.1002/pssb.201800127.
[41] A. Mariani, A. Innocenti, A. Varzi, S. Passerini, On the nanoscopic structural heterogeneity of liquid n -alkyl carboxylic acids, Phys. Chem. Chem. Phys. 23 (2021) 20282–20287, https://doi.org/10.1039/D1CP02846D.
[42] C. Massobrio, A. Pasquarello, Origin of the first sharp diffraction peak in the structure factor of disordered network-forming systems: Layers or voids?, J Chem. Phys. 114 (2001) 7976–7979, https://doi.org/10.1063/1.1365108.
[43] H.V.R. Annapureddy, H.K. Kashyap, P.M. De Biase, C.J. Margulis, What is the origin of the prepeak in the x-ray scattering of imidazolium-based room-temperature ionic liquids?, J Phys. Chem. B. 114 (2010) 16838–16846, https://doi.org/10.1021/jp108545z.

[44] H.K. Kashyap, C.J. Margulis, (Keynote) Theoretical Deconstruction of the X-ray Structure Function Exposes Polarity Alternations in Room Temperature Ionic Liquids, ECS Trans. 50 (2013) 301–307, https://doi.org/10.1149/05011.0301ecst.

[45] D.A. Keen, A comparison of various commonly used correlation functions for describing total scattering, J. Appl. Crystallogr. 34 (2001) 172–177, https://doi.org/10.1107/S0021889800019993.

[46] A. González De Castilla, J.P. Bittner, S. Müller, S. Jakobtorweihen, I. Smirnova, Thermodynamic and Transport Properties Modeling of Deep Eutectic Solvents: A Review on gE-Models, Equations of State, and Molecular Dynamics, J. Chem. Eng. Data. 65 (2020) 943–967, https://doi.org/10.1021/acs.jced.9b00548.

[47] L. Gontrani, P. Ballirano, F. Leonelli, R. Caminiti, X-Ray Diffraction Studies of Ionic Liquids: From Spectra to Structure and Back, in: R. Caminiti, L. Gontrani (Eds.), Struct. Ion. Liq., Springer International Publishing, 2014: pp. 1–37. doi:10.1007/978-3-319-01698-6.

[48] V. Migliorati, F. Sessa, P. D'Angelo, Deep eutectic solvents: A structural point of view on the role of the cation, Chem. Phys. Lett. X. 2 (2019), https://doi.org/10.1016/j.cpletx.2018.100001 100001.

[49] A. Verma, J.P. Stoppelman, J.G. McDaniel, Tuning water networks via ionic liquid/water mixtures, Int. J. Mol. Sci. 21 (2020) 403, https://doi.org/10.3390/ijms21020403.

[50] T. Steiner, Hydrogen-Bond Distances to Halide Ions in Organic and Organometallic Crystal Structures: Up-to-date Database Study, Acta Crystallogr. Sect. B Struct. Sci. 54 (1998) 456–463, https://doi.org/10.1107/S0108768197014821.

[51] G. Spoto, S. Bordiga, A. Zecchina, D. Cocina, E.N. Gribov, L. Regli, E. Groppo, C. Lamberti, New frontier in transmission IR spectroscopy of molecules adsorbed on high surface area solids: Experiments below liquid nitrogen temperature, in, Catal. Today, Elsevier (2006) 65–80, https://doi.org/10.1016/j.cattod.2005.11.011.

[52] H.W. Wilson, R.W. Macnamee, J.R. Durig, Raman spectra of gases: 24—Phenol, J. Raman Spectrosc. 11 (1981) 252–255, https://doi.org/10.1002/jrs.1250110407.